Journal of Civil Engineering and Urban Planning (2026)
Clausius Scientific Press, Canada

DOI: 10.23977/jceup.2026.080103
ISSN 2616-3969 Vol. 8 Num. 1

# *COMSOL Simulation Study on the Influence of the Parameter of the Magnetic Flux Detection Probe Receiving Coil on the Detection Performance of the Carburized Layer*

**Yang Xiao, Yingchun Chen**

*Beijing University of Technology, Beijing, China*

***Keywords:*** Non-destructive testing, Magnetic flux testing, Ethylene cracking furnace tube, Carburized layer

***Abstract:*** This study systematically investigates the precision measurement of carburized layer thickness in ethylene cracking furnace tubes. Using an induction coil probe based on magnetic flux detection as the core detection tool, and employing COMSOL Multiphysics finite element simulation, we explore the impact of receiving coil size parameters on detection performance. The feasibility of using induction coil probes for carburized layer thickness measurement is validated, providing scientific basis and technical support for practical probe manufacturing. To address the severe carburizing damage in ethylene cracking furnace tubes that jeopardizes plant safety operations and the limitations of conventional inspection methods, this study developed a two-dimensional numerical simulation model based on magnetic flux detection principles. The model integrates an induction coil probe with furnace tubes, with precise electromagnetic and structural parameters defined for each component. Using parametric scanning and single-variable analysis methods, we systematically investigated how three core dimensions-coil wire diameter, height, and outer diameter-impact detection signals. During experimental simulations, grid quality validation and normalization procedures ensured computational accuracy and reliability. These findings provide robust simulation support and theoretical foundations for optimizing structural parameters, manufacturing processes, and industrial deployment of induction coil-based carburizing layer thickness detection probes.

## 1. Introduction

As the core wear-prone component of cracking furnaces, furnace tube failure remains the primary bottleneck constraining long-term stable operation of facilities. Failure modes primarily include high-temperature creep and carburizing-induced damage. Factors such as material defects, substandard welding quality, and operational parameter fluctuations often accelerate this failure process [1]. Notably, carburizing-induced failures account for a significant proportion, posing a particularly severe threat to plant safety. Carburizing treatment significantly deteriorates the microstructure of furnace tube substrates, leading to increased hardness, abrupt decline in plasticity and toughness, and pronounced embrittlement characteristics that shorten service life [2]. Tube

fractures may critically endanger on-site operators' lives. Moreover, tube failures force unplanned shutdowns of entire ethylene plants, resulting in substantial economic losses. Concurrently, carburizing reduces cracking efficiency and increases feedstock consumption, further driving up production costs. Therefore, conducting research on carburizing damage detection for furnace tubes holds critical significance.

Pereira J M B [3] and colleagues employed a novel DC scanning magnetometer to investigate the relationship between magnetic response and furnace tube service time. Experimental results demonstrated that the instrument exhibits high sensitivity and resolution, enabling characterization of HP alloy steels under various aging conditions. Chen T. et al. [4] developed a handheld carburizing detector based on magnetic detection methods, achieving an accuracy margin of ±10%. I. C. Silva [5-7] team utilized giant magnetoresistance sensors to measure magnetic flux density in carburizing furnace tubes, establishing a micro-genetic algorithm to estimate chromium carbide volume fraction through magnetic measurements for determining carburization degree. A. C. McLeod [8,9] applied eddy current testing to analyze carburization phenomena, discovering correlation between normalized coil inductance and carburization extent. Further research revealed positive correlation between magnetic permeability changes induced by carburization and probe's normalized inductance. Arenas M P [10] integrated eddy current detection with support vector machines, employing externally magnetized saturation surfaces to classify HP heat-resistant steels under different aging states with high accuracy and reliability. Naoya Kasai et al. [11] designed a C-type probe for carburizing layer detection. By dividing test plates into oxide/nitride composite layers, acoustic layers, and carburized layers, they validated probe effectiveness through finite element analysis and experimental validation. In subsequent studies, Naoya Kasai[12] and colleagues effectively mitigated the impact of external magnetization on detection by installing a DC magnetizer outside the tube. Through finite element simulations, they established a calibration curve correlating carburization depth on the tube's outer surface with normalized inductance. Experimental validation demonstrated that this calibration curve enabled accurate determination of internal carbonization levels, which demonstrated excellent agreement with actual measurement results.

## 2. Model Establishment and Feasibility Analysis

### 2.1 Model Establishment

Table 1: Simulation Model Parameter Table

| Parameter name | unit | price |
|---|---|---|
| relative permeability of the matrix | | 1.01 |
| Matrix conductivity | S/m | $8\times105$ |
| Relative Permeability of Carburized Layer | | 20.55 |
| Conductivity of carburized layer | S/m | $3\times105$ |
| relative permeability of oxide layer | | 1.03 |
| oxidation layer conductivity | S/m | $1\times10^{-7}$ |
| Relative permeability of magnetic yoke | | 2000 |

To investigate the impact of receiving coil dimensions on detection signals, a two-dimensional numerical simulation model for evaluating carburizing layer thickness in ethylene cracking furnace tubes was developed using the COMSOL Multiphysics finite element simulation platform. In the electromagnetic field simulation environment, air was designated as the reference medium with its relative permeability baseline set to 1 to ensure consistent magnetic field calculations. To accurately characterize electromagnetic response characteristics of components under alternating

electromagnetic fields and enhance simulation accuracy, the model incorporated key electromagnetic parameters including relative permeability and conductivity for U-shaped magnetic yokes, furnace tube substrate materials, and carburizing layers of varying thicknesses, ensuring material constitutive relationships align with actual operational conditions. Detailed material parameters for each component are listed in Table 1.

The simulation model of the induction coil probe consists of five components: a U-shaped magnetic yoke, excitation coil, receiving coil, furnace tube substrate, carburized layer, and air domain. Structural parameters and material specifications for each component are rigorously aligned with actual design plans and industrial furnace tube specifications to ensure high consistency between the model and real-world operating conditions.

The U-shaped magnetic yoke beam has a cross-sectional height of 8mm, with both poles measuring 8mm in width and a 16mm spacing between them. The central crossbeam measures 32mm in length, designed to concentrate the excitation magnetic field and guide it through the furnace tube walls efficiently, thereby minimizing magnetic field loss. The excitation coil is uniformly wound around the central crossbeam of the U-shaped yoke, featuring 819 turns and a wire diameter of 0.2mm. Alternating current is applied as the excitation source, with initial settings of 1mA current and 100Hz frequency.

The receiving coils adopt a symmetrical design, evenly wound around both stimulation points of the U-shaped magnetic yoke. All receiving coils share identical specifications including turns, wire diameter, and winding density to ensure signal symmetry and consistency while minimizing system errors. Due to magnetic yoke size constraints, the coils feature a fixed inner diameter of 8mm, outer diameter of 12mm, height of 1mm, and wire thickness of 0.1mm. Center alignment between the coil and magnetic yoke poles enables precise detection of magnetic flux variations caused by carburizing layer thickness variations, ensuring measurement signals accurately reflect the carburizing layer condition.

The induction coil probe detects magnetic field variations based on electromagnetic induction principles, generating an induced voltage as its output signal. Therefore, the simulation analyzes the correlation between the induced voltage RMS value changes detected by the receiving coil and the carburized layer thickness.

The model specifies an overall furnace tube wall thickness of 8mm, with the carburizing layer simulating the actual carburizing state on the inner wall of the furnace tube. This layer adheres to the inner wall of the furnace tube base, initially set at 1mm thickness. To investigate how variations in carburizing layer thickness affect magnetic field intensity at detection points, parametric scanning was conducted with thickness parameters ranging from 1mm to 7mm in increments of 0.5mm, as shown in Figure 1.

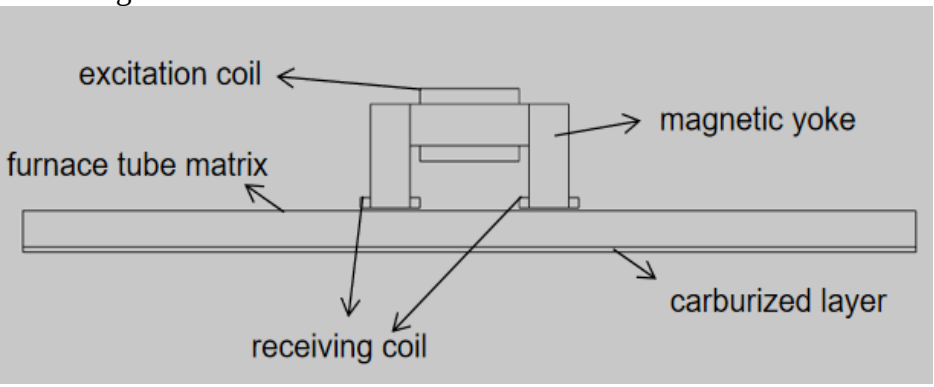


Figure 1: Simulation model of induction coil probe

The simulation model of the induction coil probe employs a free triangular meshing approach,

with differentiated mesh refinement tailored to the structural characteristics and electromagnetic properties of the components, balancing simulation accuracy and computational efficiency. As the receiving coil serves as the core detection unit of the induction coil probe, its meshing precision directly impacts the accuracy of induced voltage signal simulation. Therefore, the receiving coil area is prioritized for enhanced mesh refinement, as illustrated in Figure 2.

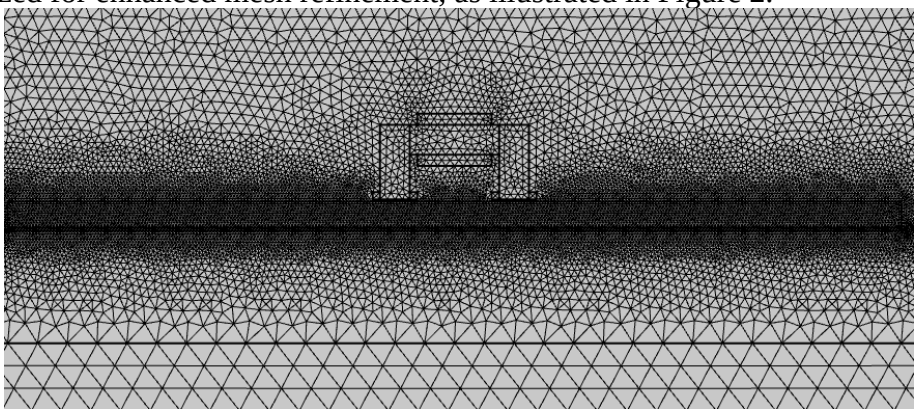

Figure 2: Meshing diagram of the induction coil probe simulation model

After grid generation, a comprehensive quality validation was performed using the COMSOL software's mesh quality analysis tool to assess metrics such as mesh distortion and aspect ratio. The mesh quality distribution of the induction coil probe simulation model is shown in Figure 3, with no abnormal meshes detected, indicating that the mesh quality meets simulation requirements.

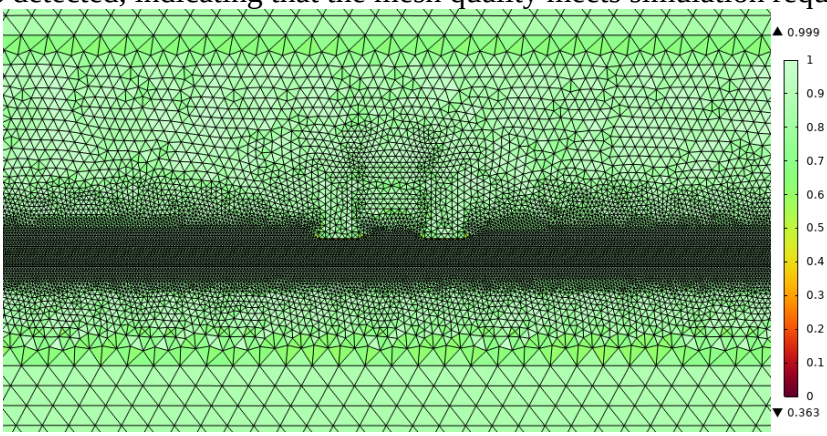


Figure 3: Grid mass distribution map of the induction coil probe simulation model

## 2.2 Simulation Results and Feasibility Analysis of Inductive Coil Probe

The simulation results shown in Figure 4 demonstrate that as the carburizing layer thickness of ethylene cracking furnace tubes progressively increases, the induction voltage of the receiving coil exhibits a distinct monotonic increasing trend. This variation pattern demonstrates excellent consistency and regularity without significant abnormal fluctuations, indicating that the induction voltage signal can stably and accurately reflect changes in carburizing layer thickness. These findings validate the feasibility of using induction coil probes for thickness detection in ethylene cracking furnace tubes.

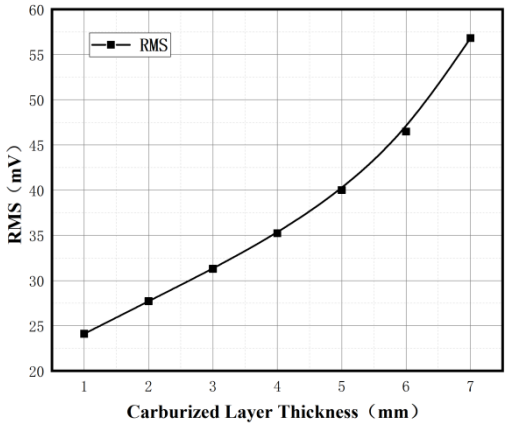


Figure 4: Effective value curve of coil induced voltage at different carburizing layer thicknesses

## 3. Study on the Impact of Receiving Coil Parameters

As the core detection component of the probe, the receiving coil serves as the primary research focus for investigating how its dimensional parameters affect magnetic field coupling efficiency, induced voltage signal characteristics, and overall detection performance, with the ultimate goal of achieving parameter optimization. The study specifically examines three critical core dimensions: wire diameter r, coil height hcoil, and outer diameter dout, while the inner diameter din has been pre-determined based on furnace tube inspection conditions. Given the clear correlation between coil winding count and these key parameters, this research systematically evaluates the impact of wire diameter, coil height, and outer diameter on detection performance. The resulting parameter optimization findings will provide reliable guidance for practical probe manufacturing processes.

The number of turns in a coil is intrinsically related to wire diameter, coil height, and coil outer diameter. Under the condition of fixed coil inner diameter, coil height and wire diameter determine the number of winding layers and single-turn arrangement density, while coil outer diameter directly limits the maximum winding turns. These three factors collectively determine the actual number of turns in the coil.

From an engineering practice perspective, the number of coil turns can be preliminarily estimated using the following formula:

$$N=\frac{h_{coil}\cdot(d_{out}-d_{in})}{2r^2}\cdot f_0 \tag{1}$$

Where $f_0$ is the coil filling factor.

The filling factor value is determined by the cross-sectional geometry of copper conductors. For tightly wound coils wound with circular copper conductors, a standard filling factor of 0.91 is typically adopted. This estimation method provides fundamental reference for parameter optimization of wire diameter, coil height, and outer coil diameter, ensuring that the optimized parameter combinations meet practical winding process requirements.

The parameter impact simulation is conducted based on the existing induction coil probe simulation model, maintaining unchanged parameters such as the U-shaped yoke structure configuration, excitation current, furnace tube and carburized layer material properties, boundary conditions, and meshing principles. By modifying only single coil parameters, the study investigates the effects on coil performance through comparative analysis of induced voltage RMS value variations under different parameter gradients, signal stability characteristics, and detection sensitivity.

### 3.1 Influence of receiving coil wire diameter

Wire diameter is a critical parameter affecting coil resistance, current carrying capacity, and winding density, directly influencing impedance characteristics and induced signal quality. To systematically investigate how receiving coil wire diameter impacts detection signal amplitude, stability, and sensitivity while clarifying the intrinsic relationship between wire diameter selection and signal characteristics, simulation experiments were conducted with wire diameters of 0.05mm, 0.1mm, and 0.2mm. To eliminate interference from other dimensional parameters such as coil outer diameter and height, single-variable control was implemented with fixed outer diameter at 12mm and height at 1mm, while maintaining all other parameters constant. This approach enabled parametric simulation studies, with simulation results subsequently normalized for consistency, as shown in Table 2.

$$U_N = \frac{U - U_{min}}{U_{min}} \tag{2}$$

where $U_N$ denotes the normalized effective voltage.

Umin = minimum effective voltage.

Table 2: Simulation parameter table for different receiving coil wire diameters

| Wire diameter (mm) | Number of coil turns | Outer diameter of coil (mm) | coil height (mm) |
|---|---|---|---|
| 0.05 | 728 | 12 | 1 |
| 0.1 | 182 | 12 | 1 |
| 0.2 | 45 | 12 | 1 |

The simulation results are illustrated in Figure 5, where Figure 5(a) shows the variation curve of the effective induced voltage with carburizing layer thickness for different receiving coil diameters, and Figure 5(b) presents the corresponding normalized effective voltage curve. As shown in Figure 5(a), under the constraints of a fixed coil outer diameter of 13mm and coil height of 1mm, the effective induced voltage of the receiving coils with all three diameters exhibits a significant monotonic increasing trend with increasing carburizing layer thickness, and the variation process is smooth without obvious fluctuations. In terms of amplitude, the influence of coil diameter on the induced voltage amplitude is highly significant, with smaller diameters resulting in higher effective voltage amplitudes.

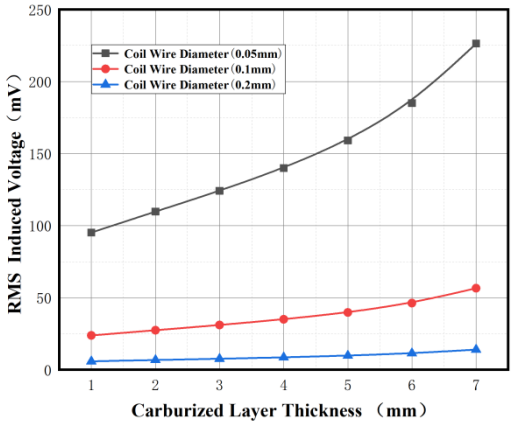


(a) Effective voltage amplitude at different receiving coil wire diameters

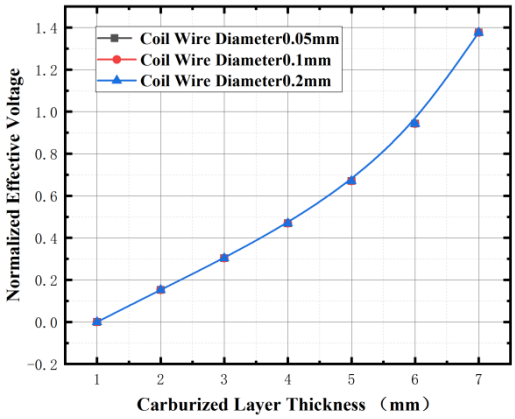


(b) Normalized effective voltage

Figure 5: Simulation calculation results of different receiving coil wire diameters

To eliminate interference from amplitude variations in detection sensitivity evaluation, normalized effective voltage measurements were performed, as illustrated in Figure 5(b). Post-normalization analysis revealed nearly complete overlap of normalized effective voltage curves across different wire diameters, indicating consistent detection sensitivity of induced voltage versus carburized layer thickness across wire diameter parameters. These findings demonstrate that wire diameter variations primarily affect induced voltage amplitude without significantly impacting probe sensitivity for carburized layer thickness measurement. While reduced wire diameters effectively enhance signal amplitude and mitigate environmental noise interference risks, they introduce process-related challenges including substantial coil resistance increases, decreased current carrying capacity, and heightened wire breakage risks during winding operations. Appropriate wire diameter enlargement effectively improves coil mechanical strength and current carrying capacity, reduces winding complexity, and consequently enhances overall probe structural stability and operational reliability.

## 3.2 Influence of receiving coil height

Table 3: Simulation parameter table for different receiving coil heights

| number | Wire diameter (mm) | Number of coil turns | Outer diameter of coil (mm) | coil height (mm) |
|---|---|---|---|---|
| 1 | 0.1 | 22 | 9 | 0.5 |
| 2 | 0.1 | 45 | 9 | 1 |
| 3 | 0.1 | 91 | 9 | 2 |
| 4 | 0.1 | 182 | 9 | 4 |
| 5 | 0.1 | 45 | 10 | 0.5 |
| 6 | 0.1 | 91 | 10 | 1 |
| 7 | 0.1 | 182 | 10 | 2 |
| 8 | 0.1 | 364 | 10 | 4 |
| 9 | 0.1 | 91 | 12 | 0.5 |
| 10 | 0.1 | 182 | 12 | 1 |
| 11 | 0.1 | 364 | 12 | 2 |
| 12 | 0.1 | 728 | 12 | 4 |
| 13 | 0.1 | 182 | 16 | 0.5 |
| 14 | 0.1 | 364 | 16 | 1 |
| 15 | 0.1 | 728 | 16 | 2 |
| 16 | 0.1 | 1456 | 16 | 4 |

To analyze how variations in receiving coil height affect coil effective voltage, the simulation parameters are specified in Table 3. All samples were divided into groups of four, with fixed key dimensions (wire diameter and coil outer diameter) within each group. The coil height was adjusted in four progressive steps: 0.5mm, 1mm, 2mm, and 4mm, followed by parameterized simulations. The calculated effective voltage amplitudes were subsequently normalized.

The simulation results shown in Figure 6 present curves depicting how normalized effective voltage of receiving coils varies with carburizing layer thickness across 16 parameter sets of coil height configurations. Notably, when maintaining constant wire diameter, coil outer diameter, and other simulation parameters, normalized effective voltage decreases with increasing coil height. Although voltage reduction occurs with height increase, all curves exhibit nearly identical slope gradients. This indicates that coil height primarily affects the amplitude level of normalized voltage, resulting in minimal impact on probe sensitivity for carburizing layer thickness detection.

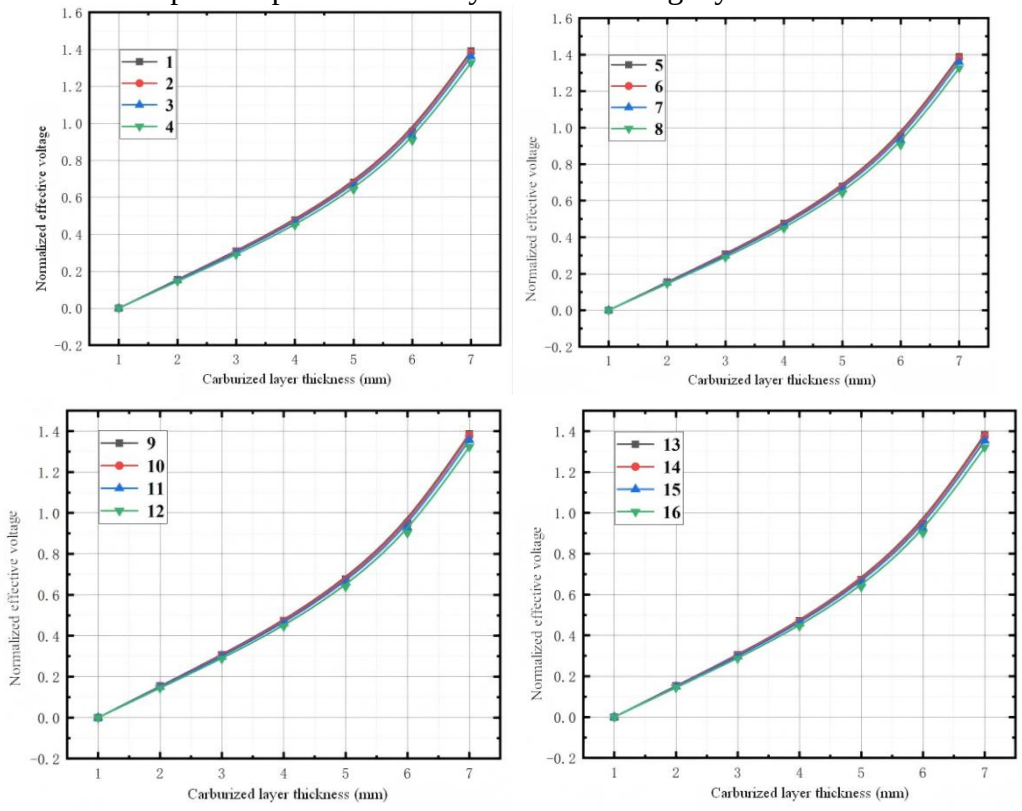


Figure 6: Simulation results of normalized effective voltage at different receiving coil heights

In summary, the primary function of coil height is to regulate the amplitude of induced voltage, which does not fundamentally affect the probe's detection sensitivity. Specifically, increasing the coil height effectively enhances the amplitude of induced voltage, improves signal noise immunity, and reduces the risk of signal suppression by ambient noise, thereby ensuring detection accuracy. However, excessive coil height not only increases the overall size of the probe, making it less suitable for industrial installation and practical operations, but also exposes the coil to electromagnetic interference from surrounding structures near the furnace tube, compromising signal stability and affecting the reliability of detection results. Conversely, reducing the coil height may decrease the probe's size and improve field adaptability, but the reduced number of coil turns lowers the amplitude of induced voltage, diminishing signal detectability and making it difficult to accurately capture subtle changes in carburized layer thickness.

### 3.3 Influence of outer diameter of receiving coil

Based on previous research findings, the receiving coil parameters including wire diameter, coil height, and inner diameter were set as follows: wire diameter 0.1mm, coil height 2mm, and inner diameter 8mm. To investigate the impact of coil outer diameter on detection performance and optimize these parameters, parametric simulation studies were conducted. The specific simulation parameters are listed in Table 4, with all results subjected to normalization processing.

Table 4: Simulation parameter table for different coil outer diameters

| number | Wire diameter (mm) | Number of coil turns | Outer diameter of coil (mm) | coil height (mm) |
|---|---|---|---|---|
| 1 | 0.1 | 91 | 9 | 2 |
| 2 | 0.1 | 182 | 10 | 2 |
| 3 | 0.1 | 364 | 12 | 2 |
| 4 | 0.1 | 728 | 16 | 2 |

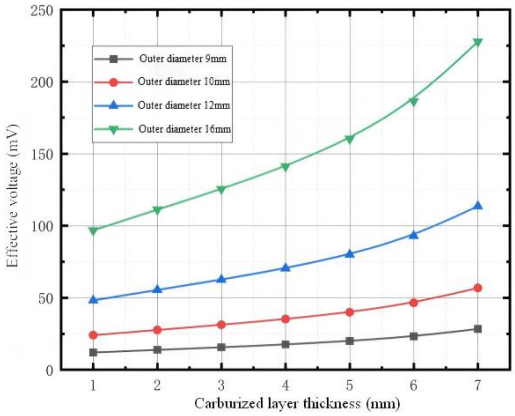


(a) Effective voltage amplitude at different outer diameters of receiving coils

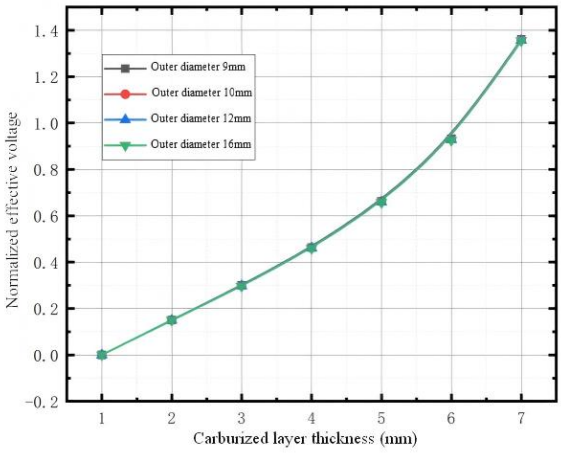


(b) Normalized effective voltage

Figure 7: Simulation results of outer diameter of different receiving coils

The simulation results are illustrated in Figure 7. Figure 7(a) shows the variation curve of effective voltage amplitude of the receiving coil with carburizing layer thickness at different outer diameters. With fixed coil dimensions (wire diameter 0.1mm, height 2mm, inner diameter 8mm) and constant carburizing layer thickness, Figure 7(a) demonstrates that effective voltage amplitude increases with outer diameter expansion. Figure 7(b) presents normalized effective voltage curves

corresponding to various outer diameters. The curves exhibit near-complete overlap across different outer diameters and show a distinct monotonic upward trend with increasing carburizing layer thickness. These findings indicate that outer diameter variations solely affect voltage amplitude amplitude without substantially influencing the probe's sensitivity in detecting carburizing layer thickness.

Through systematic research and simulation analysis of three key receiver coil size parameters-wire diameter, coil height, and outer diameter-it is concluded that these dimensions have no fundamental impact on probe detection sensitivity, primarily regulating the amplitude of induced voltage. Variations in wire diameter, coil height, and outer diameter lead to corresponding increases or decreases in induced voltage amplitude, thereby affecting signal anti-interference capability and detectability. However, these changes do not alter the slope of induced voltage variation with carburizing layer thickness, meaning they maintain the probe's responsiveness to subtle thickness variations. Since parameter selection focuses solely on probe volume compatibility and induced voltage amplitude requirements, optimal size parameters can be determined by balancing detection signal amplitude specifications with practical considerations such as on-site probe adaptability and manufacturing processes.

## 4. Conclusion

This study focuses on an induction coil-type magnetic flux detection probe for carburizing layer thickness measurement. Through COMSOL Multiphysics finite element simulation, we systematically investigated the impact of receiving coil size parameters on detection performance, elucidating the functional relationships of each parameter. The key findings include:

(1) The simulation model of induction coil probes based on magnetic flux detection principles accurately replicates the thickness measurement process of carburizing layers in ethylene cracking furnace tubes. Simulation results demonstrate that the effective value of induced voltage in receiving coils exhibits a stable monotonic increasing trend with increasing carburizing layer thickness, showing no significant abnormal fluctuations. This validates the feasibility of using induction coil probes for thickness detection in ethylene cracking furnace tubes, providing a reliable simulation foundation for subsequent probe design and optimization.

(2) The impact of receiving coil wire diameter on detection signals is primarily reflected in the amplitude of induced voltage. Smaller wire diameters result in higher induced voltage amplitudes, but reduced wire diameter increases coil winding difficulty, decreases mechanical strength, and reduces current carrying capacity. The normalized effective voltage curves corresponding to different wire diameters are essentially overlapping, indicating that wire diameter has no significant effect on detection sensitivity.

(3) The receiving coil height only affects the amplitude of induced voltage and has no intrinsic correlation with detection sensitivity. Increasing the coil height can enhance the amplitude of induced voltage and improve anti-interference capability, but it may increase probe volume and susceptibility to electromagnetic interference. Reducing the coil height can minimize probe volume and improve field adaptability, but it may decrease signal detectability. A balanced selection should be made based on actual operating conditions.

(4) Variations in the outer diameter of the receiving coil only modulate the amplitude of the induced voltage without altering detection sensitivity. The larger the outer diameter of the coil, the higher the induced voltage amplitude. Under the premise of ensuring on-site compatibility of the probe and feasibility of manufacturing processes, signal amplitude optimization can be achieved by adjusting the outer diameter of the coil.

In summary, the three core dimensional parameters of the receiving coil solely affect the

amplitude of the induced voltage without altering the probe's sensitivity in detecting carburizing layer thickness. During practical probe design and fabrication, optimal parameters can be selected by balancing signal amplitude requirements with practical considerations such as industrial installation compatibility, winding process complexity, and structural stability. This research provides crucial theoretical support and simulation data for the engineering application of induction coil-based carburizing layer thickness detection probes, significantly enhancing the accuracy and reliability of carburizing layer inspection in ethylene cracking furnace tubes.

## References


*[1] Wu Jianping. Analysis of failure causes and countermeasures for radiation section furnace tubes in ethylene cracking furnaces [J]. Petroleum and Chemical Equipment, 2013, 16(08): 30-33*

*[2] Jin Peibin, Shen Limin. Research progress on failure modes and cause analysis of ethylene cracking furnace tubes [J]. Chemical Machinery, 2016,43(03):263-267+301.*

*[3] Pereira J M B, Pacheco C J, Arenas M P, et al. Novel scanning dcsusceptometer for characterization of heat-resistant steels with different states of aging[J]. Journal of Magnetism and Magnetic Materials, 2017, 442: 311-318.*

*[4] CHEN T, CHEN X, CHEN J, et al. Magnetic method for rapid detection of carburization degree of Fe-Cr-Ni series hightemperature heat-resistant alloy [J]. Journal of Pressure Vessel Technology, 2022,144(5):051504.*

*[5] I. C. da Silva, R.S. da Silva, J.M.A. Rebello, et al. Characterization of carburization of HP steels by non destructive magnetic testing[J]. NDT & E International, 2006, 39(7): 569-577.*

*[6] I.C. Silva, L.L. Silva, R.S. Silva, et al. Carburization of ethylene pyrolysis tubes determined by magnetic measurements and genetic algorithm[J]. Scripta Materialia, 2007, 56(4): 317-320.*

*[7] I.C. Silva, J.M.A. Rebello, A.C. Bruno, et al. Structural and magnetic characterization of a carburized cast austenitic steel[J]. Scripta Materialia, 2008, 59(9): 1010-1013.*

*[8] A. C. McLeod, C. M. Bishop, K. J. Stevens, et al. Microstructure and Carburization Detection in HP Alloy Pyrolysis Tubes[J]. Metallography, Microstructure, and Analysis, 2015, 4(4): 273-285*

*[9] A. C. McLeod, C. M. Bishop, K. J. Stevens, et al. Microstructural Characterization and Image Analysis in Ex-Service HP Alloy Stainless Steel Tubes for Ethylene Pyrolysis[J]. Metallography, Microstructure, and Analysis, 2016, 5(3): 178-187*

*[10] Arenas M P, Rocha T J, Angani C S, et al. Novel austenitic steel ageing classification method using eddy current testing and a support vector machine[J]. Measurement, 2018, 127: 98-103*

*[11] Naoya Kasai, Syuji Ogawa, Toshiyuki Oikawa, et al. Detection of Carburization in Ethylene Pyrolysis Furnace Tubes by a C Core Probe with Magnetization[J]. Journal of Nondestructive Evaluation, 2010, 29(3): 175-180.*

*[12] Katsunobu Hasegawa, Toshiyuki Oikawa, Naoya Kasai. Development of an Eddy Current Inspection Technique with Surface Magnetization to Evaluate the Carburization Thickness of Ethylene Pyrolysis Furnace Tubes[J]. Journal of Nondestructive Evaluation, 2012, 31(4): 349-356.*